



Turbulent rectangular compound open channel flow study using multi-zonal approach

Jaan H. Pu¹ 

Received: 10 September 2018 / Accepted: 12 December 2018
© The Author(s) 2018

Abstract

In this paper, an improved Shiono–Knight model (SKM) has been proposed to calculate the rectangular compound open channel flows by considering a multi-zonal (MZ) approach in modelling turbulence and secondary flows across lateral flow direction. This is an effort to represent natural flows with compound shape more closely. The proposed model improves the estimation of secondary flow by original SKM model to increase the accuracy of depth-averaged velocity profile solution formed within the transitional region between different sections (i.e. between main-channel and floodplain) of compound channel. This proposed MZ model works by sectioning intermediate zones between floodplain and main-channel for running computation in order to improve the modelling accuracy. The modelling results have been validated using the experimental data by national UK Flood Channel Facility. It has been proven to work reasonably well to model secondary flows within the investigated compound channel flow cases and hence produce better representation to their flow lateral velocity profile.

Keywords Shiono–Knight method · Secondary flow · Turbulence · Natural flow · Lateral velocity distribution · Depth-averaged model

List of symbols

b	Half of the in-bank channel width (m)
B	Half of the whole channel surface width (m)
D_r	Relative depth (–)
f	Friction factor (–)
g	Gravitational acceleration (m/s^2)
h	Height of in-bank channel (m)
H	Flow depth (m)
S_o	Bed slope (–)
t	Time (s)
U_*	Shear velocity (m/s)
U	Velocity in x direction (m/s)

✉ Jaan H. Pu
j.h.pu1@bradford.ac.uk

¹ School of Engineering, Faculty of Engineering and Informatics, University of Bradford, Bradford DB7 1DP, UK

U_d	Depth-averaged velocity (m/s)
U_w	Width-averaged velocity (m/s)
V	Velocity in y direction (m/s)
W	Velocity in z direction (m/s)
x	Streamwise coordinate (m)
X	Water body forces (Pa)
y	Lateral coordinate (m)
z	Coordinate normal to bed (m)
ρ	Density of water (kg/m^3)
τ	Shear stress (Pa)
μ	Kinematic viscosity (m^2/s)
σ	Normal stresses (Pa)
ε	Eddy viscosity (kg/ms)
Γ	Secondary flow parameter ($\text{kg}/(\text{ms}^2)$)
λ	Dimensionless eddy viscosity ($-$)
$\bar{\varepsilon}_{yx}$	Depth-averaged eddy viscosity (m^2/s)
τ_b	Local boundary shear stress (Pa)

1 Introduction

In recent years, studies into compound channels have been undertaken due to its importance in representing the seasonal-impact rivers and floodplains. The naturally formed compound channel usually consisted of a deeper main-channel known as the in-bank and shallower floodplains known as the over-bank. This un-even channel could affect the flow velocity distribution, which could alter its sediment transport pattern [8]. In order to represent these flows, Shiono and Knight [11] introduced an analytical Shiono–Knight model (SKM) based on the simplified two-dimensional (2D) Reynolds Averaged Navier–Stokes (RANS) equations. The model ignored the effect of turbulence created from secondary currents. The SKM was improved when Shonio and Knight [12] included the effects of secondary flows within the SKM model, which they also found that the turbulence and secondary flow occurrences are complicated in compound channel flows due to the lateral exchange of flow momentum between the main-channel and floodplains.

Some compound channel studies further considered the channel-shape-generated turbulence as well as secondary flows to improve flow velocity profile representation (i.e. Ervine et al. [2] and Tang and Knight [13]). Studies by Yang et al. [17] showed that large-scale eddies are formed by instability in regions with high velocity variation, such as at the interface between main-channel and its floodplains of a compound channel flow. All these studies showed that the accurate calculation of secondary currents and hence turbulence are crucial for estimating the flow velocity.

To ease the consideration of secondary flows in SKM model, Shonio and Knight [12] assigned a secondary flow parameter, Γ , into their model to calculate flow velocity, where this approach was commonly adopted in later studies [13–15, 18]. The parameter was chosen to represent each section in those studies to ensure the appropriate flow representation at main-channel and floodplain. Liao and Knight [3] and [4] further investigated Γ together with local friction factor (f) and dimensionless eddy viscosity (λ) for trapezoidal and rectangular compound channels respectively. They proved the importance of all these parameters in SKM model, in particular Γ . From their studies, it has been proposed that

velocity profile mis-representation could happen due to secondary flow assumption used by the SKM model. This mis-representation error usually occurs due to the lumping of single parameter within a section (i.e. within main-channel or floodplain) as a simplifying step at SKM modelling. Tang and Knight [13] considered the SKM's boundary conditions associated with complex compound geometries and proved that by modifying SKM its velocity profile calculation can be improved for flows with different aspect ratios. Consequently, in Tang and Knight [14], it has been acknowledged that there is a lack of experimental and theoretical understanding to Γ which can lead to the inaccuracy of velocity computation.

In Tang and Knight [15], several analytical models have been reviewed and further tested, including by Ervine et al. [2], Castanedo et al. [1] and Van Prooijen et al. [16]. Ervine et al. [2] based their model by assuming the temporal-mean transverse velocity component in the flow momentum equation to be fraction of the streamwise depth-averaged velocity U_d , hence replacing Γ by KU_d^2 , where K is a weighted coefficient. In their model, K was used to account for complex 3D interfacing of the main-channel and floodplain, which includes the effect of horizontal shear layer, mass exchange in and out of each section and any expansion and contraction losses from non-prismatic channels. In Castanedo et al. [1], three different forms of the turbulent shear stress were investigated, however their model did not take into account the secondary flow effect. Van Prooijen et al. [16] proposed an analytical eddy viscosity model that included the effects of the horizontal coherent structures as well as the effects of 3D wall-induced turbulence. Tang and Knight [15] suggested that the large horizontal eddies induced by strong shearing in the sections' mixing region play a significant role in the flow transverse mixing process. As a result, various eddy viscosity models that take into account the horizontal coherent structures and turbulence (i.e. Van Prooijen et al. [16]) have shown promising modelling outcomes.

From studies above, the turbulence and secondary flow are identified to be crucial for analytical model to represent velocity profile reasonably. The key forming of secondary flow usually takes place at the interval between sections (i.e. between main-channel and floodplain) of compound channel where its effect towards velocity is hard to be modelled accurately. Shiono and Knight [12] and Tang and Knight [13] have suggested that more complex sub-divided section members within a compound channel may be able to improve velocity modelling accuracy, but there is complexity to represent additional section's turbulence and secondary flow. Due to this, a novel multi-zonal (MZ) model is proposed and investigated in this study for its suitability to improve common SKM model to represent velocity profile across rectangular compound channel. The proposed MZ model utilises extra section to improve the modelling of turbulence and secondary flow within the investigated compound channel flows and hence enhance the accuracy of velocity profile calculation. The proposed model has also been validated against the UK Flood Channel Facility (FCF) experimental data.

2 Model descriptions

2.1 Shiono–Knight (SKM) and turbulence modelling

Originated from the SKM model by Shiono and Knight [11, 12], Castanedo et al. [1] and Van Prooijen et al. [16] has proposed methods to improve the SKM's turbulence modelling. However, their respective comparisons with experimental data demonstrated that the flow modelling improvement mainly restricted to flow regions away from compound sections' interval.

Yang et al. [18] considered a model attempting to represent flow velocity profile in rectangular compound channel. Their proposal was different to the SKM at designing secondary flows and eddy viscosity by considering momentum transfer.

Consequently, it appears that several studies for the compound channel flows were based around modifying the SKM model due to its modelling capability. Their proposed modifications to the SKM presented improved results from the original SKM model suggesting its versatility to adapt to different improved functions. Ergo, in this study, the SKM model will be adapted and improved.

The proposed governing model from Navier–Stokes equations suggested by Shiono and Knight [11] SKM model can be described as follows

$$\rho X + \frac{\partial \sigma_{xx}}{\partial x} + \frac{\partial \tau_{yx}}{\partial y} + \frac{\partial \tau_{zx}}{\partial z} = \rho \left(U \frac{\partial U}{\partial x} V \frac{\partial U}{\partial y} + W \frac{\partial U}{\partial z} + \frac{\partial U}{\partial t} \right) \tag{1}$$

where ρ is water density; X is water body force; τ is shear stress; σ is normal stress; x , y and z denote streamwise, lateral and vertical directions; t denotes time; and U , V and W are velocity at x , y and z -direction. The subscripts for τ and σ indicate their acting direction.

In order to form the governing equation for lateral variation of depth-averaged velocity, U_d , the depth-averaged momentum equation has to be solved for steady uniform turbulent flow in the streamwise direction. And by considering the dominant horizontal eddies across the channel, one can get that $\partial U / \partial x = \partial \sigma_{xx} / \partial x = 0$. Furthermore, it is assumed that the velocity variation is steady i.e. $\partial U / \partial t = 0$. As a result, the governing equations becomes (when combined with the continuity equation)

$$\rho H \frac{\partial}{\partial y} (UV) = \rho g S_o H + \frac{\partial \tau_{yx}}{\partial y} H + \frac{\partial \tau_{zx}}{\partial z} H \tag{2}$$

where H is water flow depth.

Combining the bed shear stress theory with the Darcy-Weisbach equation, the following equation can be deduced

$$\frac{\partial \tau_{zx}}{\partial z} = \frac{f U_d^2 \rho}{8H} \tag{3}$$

where f is friction factor.

Shiono and Knight [12] stated that the depth-averaged transverse shear stress τ_{yx} can be expressed in terms of lateral gradient of U_d as

$$\tau_{yx} = \rho \bar{\epsilon}_{yx} \frac{\partial U_d}{\partial y} \tag{4}$$

where

$$\bar{\epsilon}_{yx} = \lambda U_* H \tag{5}$$

and $\bar{\epsilon}_{yx}$ is depth-averaged eddy viscosity; λ is dimensionless eddy viscosity; and U_* is shear velocity.

Substituting the above into the Eq. (2) together with using the expression of shear velocity $U_* = (\tau_b / \rho)^{\frac{1}{2}}$, we could deduce that

$$\frac{\partial}{\partial y} [H(\rho UV)_d] = \rho g S_o H - \frac{f \rho U_d^2}{8} + \frac{\partial}{\partial y} \left\{ \rho \lambda H^2 \left(\frac{f}{8} \right)^{\frac{1}{2}} U_d \frac{\partial U_d}{\partial y} \right\} \tag{6}$$

where τ_b is the local boundary shear stress; and subscript d denotes depth-averaged characteristic of a parameter.

The secondary flows in the depth-averaged Eq. (6) can be assumed as follows [12, 13]

$$\frac{\partial}{\partial y} [H(\rho UV)_d] = \Gamma \tag{7}$$

In uniform flow, the depth-averaged velocity equation can be expressed as follows [from Eqs. (6)–(7)]

$$U_d = [A_1 e^{\gamma y} + A_2 e^{-\gamma y} + k]^{\frac{1}{2}} \tag{8}$$

where

$$k = \frac{8gS_oH}{f}(1 - \beta) \tag{9}$$

in which

$$\beta = \frac{\Gamma}{\rho g S_o H} \text{ and } \gamma = \sqrt{\frac{2}{\lambda}} \left(\frac{f}{8}\right)^{\frac{1}{4}} \frac{1}{H} \tag{10}$$

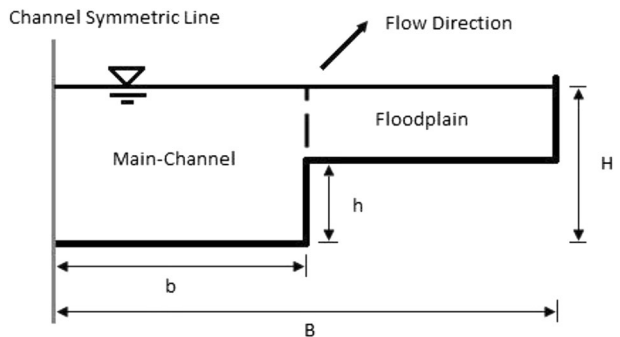
In Eqs. (8)–(10), Γ is secondary flow parameter; S_o is bed slope; g is gravitational acceleration; and A_1, A_2, k, β and γ are all coefficients used for depth-averaged velocity formulation.

2.2 Boundary conditions

The schematic diagram for the rectangular compound channel flow is showing at Fig. 1, where it consists of two sections within the channel: deeper main-channel and shallower floodplain. Liao and Knight [3, 4] discussed the boundary conditions produced by compound channel in which they suggested each section should possess separate constants Γ, f and λ . This is because the velocity at the main-channel and floodplain is not continuous but affected from the region where the sections meet. They further proposed that

$$\left. \frac{\partial U_d^{(1)}}{\partial y} \right|_{y=0} = 0 \tag{11}$$

Fig. 1 Rectangular compound channel and dimensions



$$U_d^{(2)} \Big|_{y=B} = 0 \tag{12}$$

The superscript in each boundary refers to the section number (i.e. 1 for main channel and 2 for floodplain). By approximating this relationship using proportional approach, Liao and Knight [3] produced

$$Ud^{(2)} \approx \alpha_u Ud^{(1)} \tag{13}$$

where the following relationships can describe α_u at Eq. (13) above

$$\frac{\alpha_u b}{B} = K_u D_r + B_u \tag{14}$$

in which

$$D_r = (H - h)/H \tag{15}$$

$$K_u = -0.123601 \left(\frac{B}{b}\right)^2 + 0.518198 \left(\frac{B}{b}\right) + 0.019269 \tag{16}$$

$$B_u = 0.0179595 \left(\frac{B}{b}\right)^2 - 0.166066 \left(\frac{B}{b}\right) + 0.600033 \tag{17}$$

α_u, K_u, B_u are coefficient constants; D_r is relative depth [as showing at Eq. (14)]; and B, b and h are half of the whole channel surface width, half of the in-bank channel width and flow depth at in-bank channel respectively (as can be referred to Fig. 1).

Therefore, from Eq. (13), the boundary conditions at $y=b$ can be written as

$$\alpha_u U_d^{(1)} \Big|_{y=b} = U_d^{(2)} \Big|_{y=b} \tag{18}$$

$$\frac{\partial U_d^{(1)}}{\partial y} \Big|_{y=b} = \frac{\partial U_d^{(2)}}{\partial y} \Big|_{y=b} \tag{19}$$

After all four boundary conditions at Eqs. (11), (12), (18) and (19) are applied into Eq. (8), A coefficients become

$$A_1 = A_2 = \frac{A_3 \gamma_2 e^{\gamma_2 b} - A_4 \gamma_2 e^{-\gamma_2 b}}{2 \gamma_1 \alpha_u \sinh(\gamma_1 b)} \tag{20}$$

where

$$A_3 = -C_2 e^{-\gamma_2 B} - A_4 e^{-2\gamma_2 B} \tag{21}$$

$$A_4 = \frac{C_2 - \alpha_u^2 C_1 + [\alpha_u \gamma_2 C_2 e^{\gamma_2 (b-B)}] / [\gamma_1 \tanh(\gamma_1 b)] - C_2 e^{\gamma_2 (b-B)}}{e^{\gamma_2 (2b-B)} - e^{-\gamma_2 b} - [\alpha_u \gamma_2 e^{\gamma_2 (b-2B)}] / [\gamma_1 \tanh(\gamma_1 b)] - (\alpha_u \gamma_2 e^{-\gamma_2 b}) / [\gamma_1 \tanh(\gamma_1 b)]} \tag{22}$$

in which, $A_3, A_4, C_1, C_2, \gamma_1$ and γ_2 are all coefficients for SKM boundary conditions.

In Eqs. (20)–(22), A_1 and A_2 are related to the symmetrical and wall-slip conditions of the channel, whereas their associated A_3 and A_4 are related to flow continuity between sections. Substituting A coefficients into the depth-averaged velocity equation gives

$$Ud^{(1)} = \sqrt{2A_1 \cosh(\gamma_1 y) + C_1} \tag{23}$$

$$Ud^{(2)} = \sqrt{A_3 e^{\gamma_2 y} + A_4 e^{-\gamma_2 y} + C_2} \tag{24}$$

where

$$C_1 = \frac{8gSoH}{f_1}(1 - \beta_1), \quad C_2 = \frac{8gSo(H - h)}{f_2}(1 - \beta_2), \quad \beta_1 = \frac{\Gamma_1}{\rho g So H}, \quad \text{and} \quad \beta_2 = \frac{\Gamma_2}{\rho g So(H - h)} \tag{25}$$

3 New multi-zonal model and its validations

3.1 Modelling parameters

In analytical modelling, the parameters for secondary flow and eddy viscosity are crucial to ensure a precise representation to the compound channel flows. As proven in the calibration processes by Shiono and Knight [12], Tang and Knight [13, 14, 15], and Liao and Knight [3, 4], those parameters significantly influenced the performance of modelling calculation, in particular at near-wall and section transitional regions. Through the calibration using the UK-FCF experimental data, this study obtains a set of calibrated secondary flow and dimensionless eddy viscosity parameters. As for the friction factor, it has been obtained using the measured shear stress in the experiment, hence same coefficients used by the SKM model will be employed in this study [3, 14].

In Figs. 2, 3, 4, 5, 6 and 7, the results of the proposed secondary flow and dimensionless eddy viscosity parameters are compared to the UK-FCF experimental data for rectangular

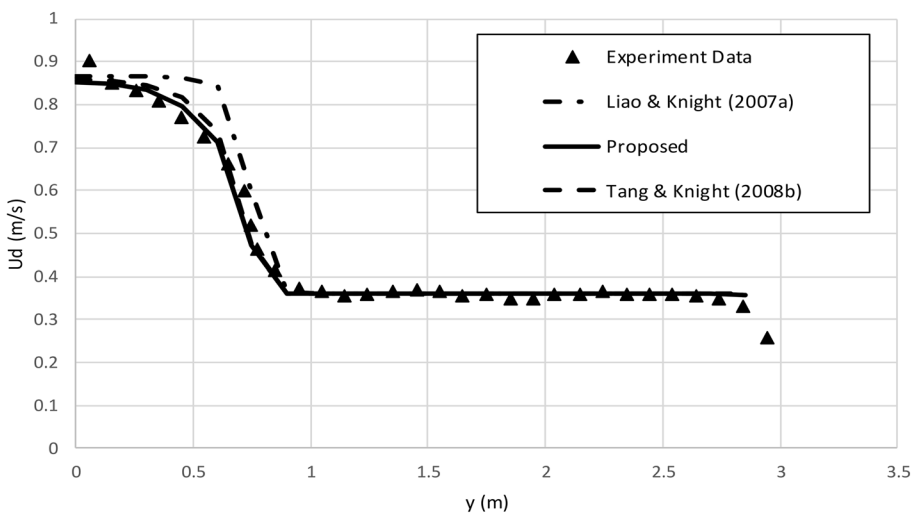


Fig. 2 FCF0804 depth-averaged velocity comparison between the proposed model and literatures

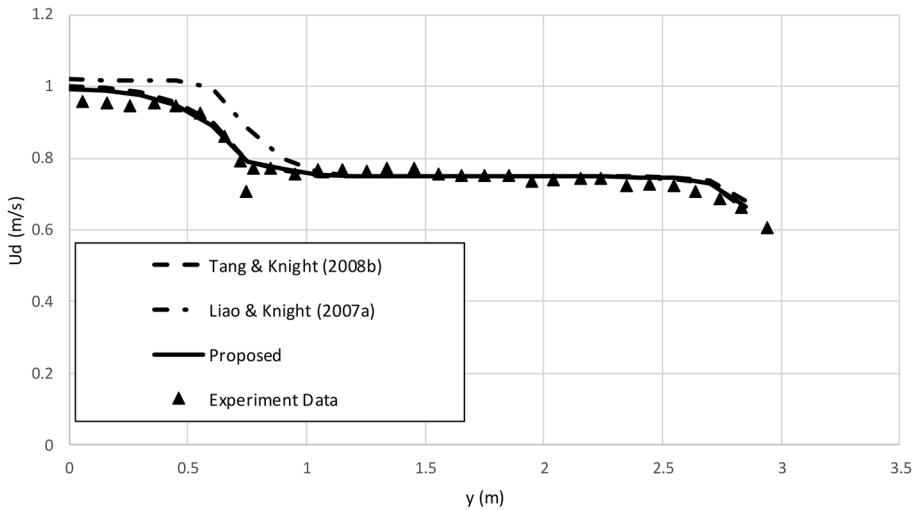


Fig. 3 FCF0807 depth-averaged velocity comparison between the proposed model and literatures

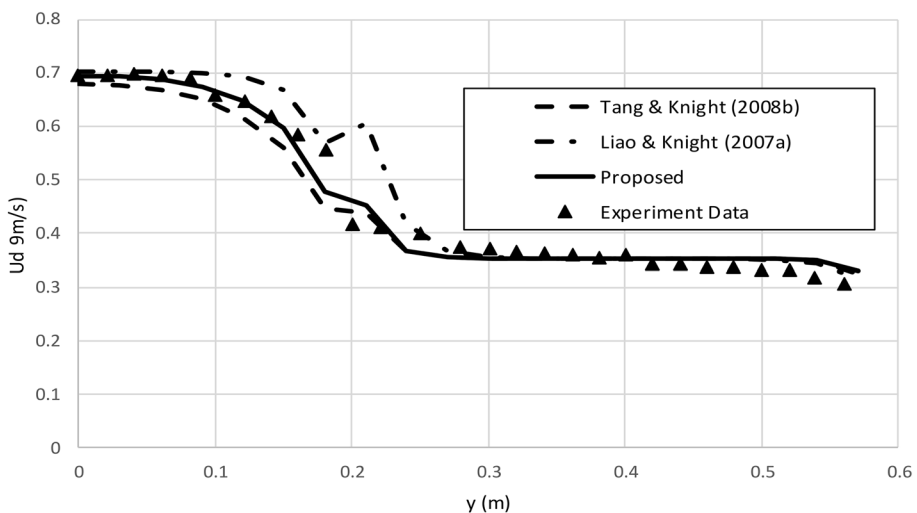


Fig. 4 ROS224 depth-averaged velocity comparison between the proposed model and literatures

compound channel flows. The experimental conditions and width-averaged velocity (U_w) for tests in Figs. 2, 3, 4, 5, 6 and 7 are described in Table 1, where the utilised B/H aspect ratio range from 1.98 to 15.99. For comparison purpose, the models by Tang and Knight [14], and Liao and Knight [3] are also plotted in same Figs. 2, 3, 4, 5, 6 and 7.

It can be observed from the figures that the proposed parameter set gives reasonable representation to the experimental data, especially at the main-channel flow region. However, it has not presented adequate representation to the measurements at interface region between main-channel and floodplain, except for a few flow cases. The models by Tang and Knight [3, 14] have also shown non-precise representation to the measured velocity profile

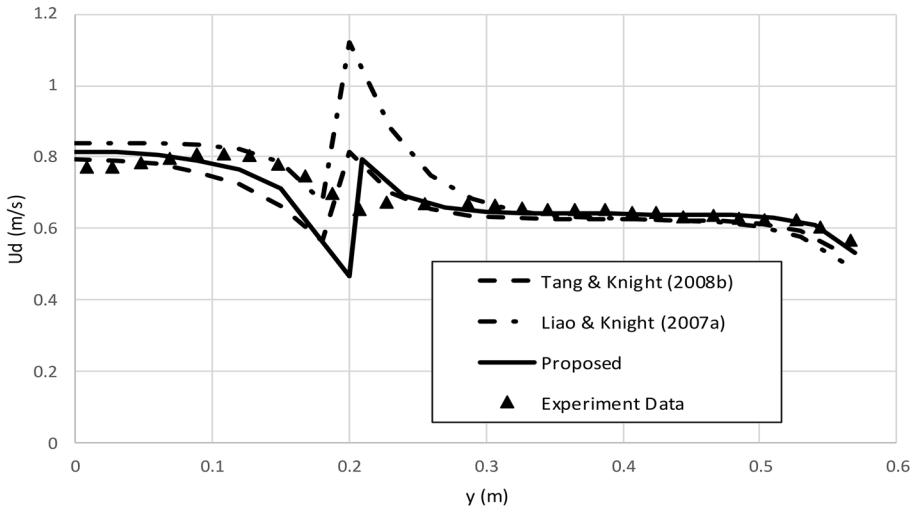


Fig. 5 ROS245 depth-averaged velocity comparison between the proposed model and literatures

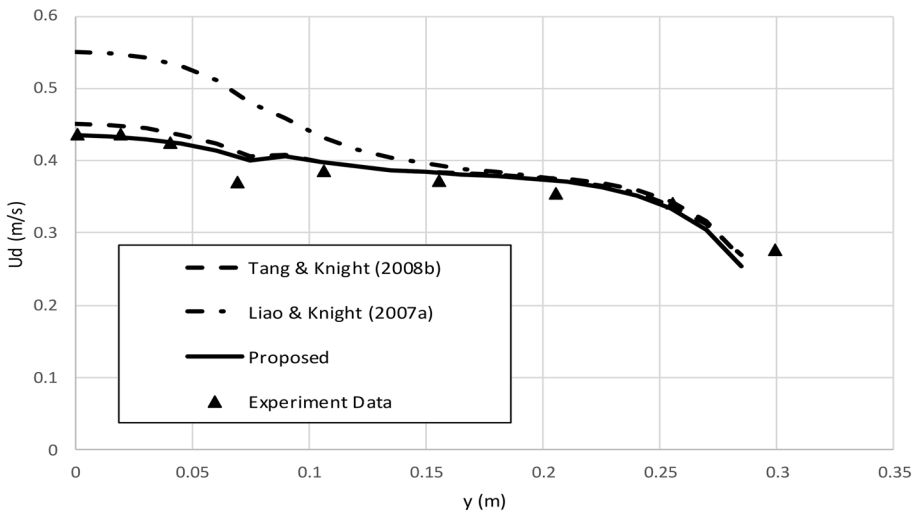


Fig. 6 DWK0404 depth-averaged velocity comparison between the proposed model and literatures

at the main-channel and floodplain interface. To further compare the proposed parameter sets with suggestions from Tang and Knight [14] and Liao and Knight [3], Table 2 has been produced. From the table, it can be observed that the proposed calibrated parameters fall within a reasonable range to those suggested in literatures.

From the model validation process, it has been found that the flow tests with high aspect ratio of B/H (i.e. FCF0804, FCF0807 and ROS224) can be represented quite accurately by SKM models (by Liao and Knight [3] and Tang and Knight [14]), and by the present calibrated model. For other flow tests with smaller B/H ratios, all models show incapability to represent the compound channel flows with high accuracy. The key

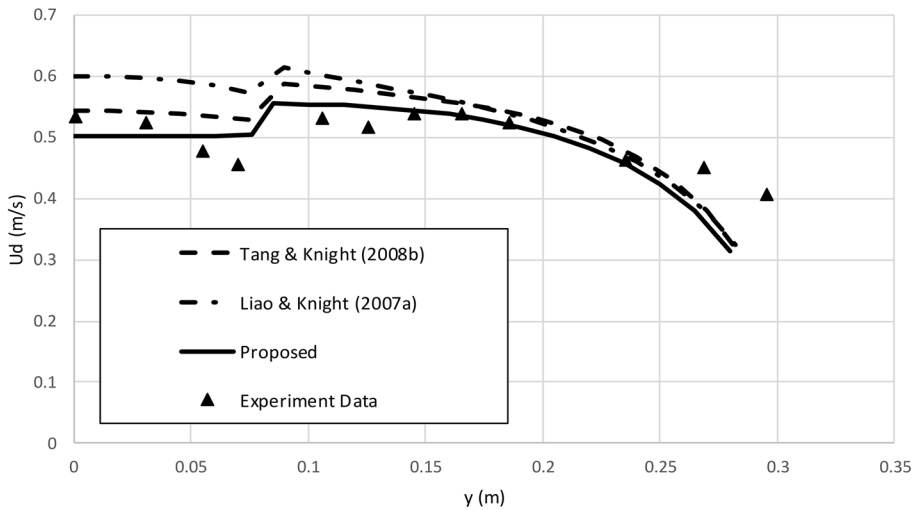


Fig. 7 DWK0406 depth-averaged velocity comparison between the proposed model and literatures

Table 1 Experimental conditions for compound channel flow tests

Experiment no.	B/H (-)	S_o (-)	b (m)	h (m)	B (m)	H (m)	U_w (m/s)
FCF0804	15.99	0.001027	0.750	0.150	3.00	0.18760	0.469
FCF0807	11.99	0.001027	0.750	0.150	3.00	0.25020	0.783
ROS224	8.37	0.002024	0.400	0.050	0.60	0.07165	0.464
ROS245	6.93	0.002024	0.400	0.050	0.60	0.08660	0.692
DWK0404	2.67	0.000966	0.076	0.076	0.30	0.11420	0.379
DWK0406	1.98	0.000966	0.076	0.076	0.30	0.15380	0.497

Table 2 Coefficients summary for compound channel flow tests

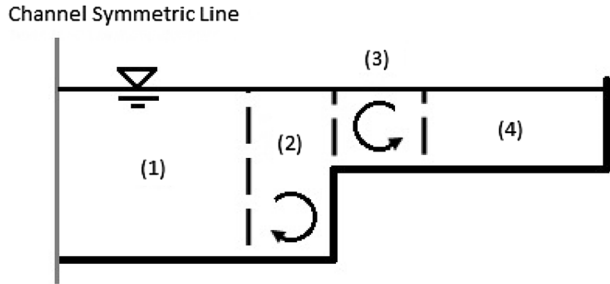
Experiment no.	B/H	Tang and Knight [14]		Liao and Knight [3]		Present study	
		λ (1&2)	Γ (1&2)	λ (1&2)	Γ (1&2)	λ (1&2)	Γ (1&2)
FCF0804	15.99	0.07, 0.07	0.25, -0.10	0.01, 0.10	0.25, -0.15	0.10, 0.09	0.30, -0.095
FCF0807	11.99	0.08, 0.07	0.60, -0.25	0.01, 0.10	0.25, -0.15	0.10, 0.09	0.65, -0.25
ROS224	8.37	0.07, 0.07	0.25, -0.10	0.01, 0.10	0.25, -0.15	0.035, 0.055	0.24, -0.10
ROS245	6.93	0.07, 0.07	0.35, -0.25	0.01, 0.10	0.25, -0.15	0.035, 0.055	0.40, -0.30
DWK0404	2.67	0.07, 0.07	0.34, -0.092	0.01, 0.10	0.25, -0.15	0.10, 0.09	0.39, -0.091
DWK0406	1.98	0.03, 0.07	0.55, -0.187	0.01, 0.10	0.25, -0.15	0.10, 0.09	0.60, -0.18

inaccuracy happens at the flow interface between main-channel and floodplain prompting the use of different approach to model this region of flow is needed. The following section will describe a new multi-zonal (MZ) approach to improve compound channel study.

Table 3 Experimental conditions for flows with small aspect ratios for multi-zonal (MZ) model tests

Experiment no.	B/H (-)	S _o (-)	b (m)	h (m)	B (m)	H (m)	U _w (m/s)
DWK0406	1.98	0.000966	0.076	0.076	0.30	0.1538	0.497
ROS255	6.36	0.002024	0.400	0.050	0.60	0.0950	0.783
ROS250	6.55	0.002024	0.400	0.050	0.60	0.0920	0.738
ROS245	6.93	0.002024	0.400	0.050	0.60	0.0866	0.692
ROS240	7.10	0.002024	0.400	0.050	0.60	0.0846	0.674

Fig. 8 Secondary flow components at interface zone between main-channel and floodplain. (1)–(4) represent zones within the compound channel flow



3.2 Proposed multi-zonal (MZ) approach

As proven in the previous section, some compound channel flows have not been represented precisely by SKM approach in particular flows with small aspect ratio. Motivated by this fact, a multi-zonal (MZ) approach has been proposed in this study to improve the flow modelling at the interface flow region between floodplain and main-channel. The UK-FCF experiments with small aspect ratio of B/H and flow depth H are benchmarked to find out the accuracy of the proposed MZ model. These small aspect ratio tests include various ROS and DWK flow cases, where their flow conditions and U_w are outlined at Table 3. All tests in this section have aspect ratio from 1.98 to 7.10.

The MZ model works by sectioning out an additional zone in the interface between floodplain and main-channel. To model this zone, the MZ model will consider stronger secondary flow created at the step of compound channel and implement this additional impact into β for SKM modelling, which is presented at the following Eqs. (26)–(27). Fundamentally, the secondary flow at compound step consists of two components acting in opposed manner to each other (refer to schematic diagram at Fig. 8), as suggested in Nezu and Nakagawa [5]. By considering these components of secondary flow, the SKM calculation could be improved and hence the consideration of U_d.

$$\beta'_1 = \frac{\Gamma'_1}{\rho g S_o H} \tag{26}$$

$$\beta'_2 = \frac{\Gamma'_2}{\rho g S_o (H - h)} \tag{27}$$

where, β'_1 and β'_2 are coefficients at zones 2 and 3 within the flow interface area (showing at Fig. 8 below); and $\Gamma'_1 = \Gamma_1 + \varphi_1$ and $\Gamma'_2 = \Gamma_2 + \varphi_2$, in which φ_1 and φ_2 represent the Γ components due to the escalated secondary flow at zones 2 and 3 within the flow interface area.

It has been found in this study that the interface zones 2 and 3 in Fig. 8 are accounted for about 10-25% of the distance for main-channel and floodplain respectively (agreed with findings by experimental studies on various channel flows in [6, 10]). In comparison, the shallower zone 3 is lengthier than zone 2 as the secondary flow has less depth of water to evolve vertically. Since both secondary flow φ_1 and φ_2 components act at the counter-rotational manner, they are estimated to have positive and negative impact to Γ'_1 and Γ'_2 respectively. In the exact middle of the meeting point between main-channel and floodplain, φ_1 and φ_2 are set at zero as both secondary flow components neutralised.

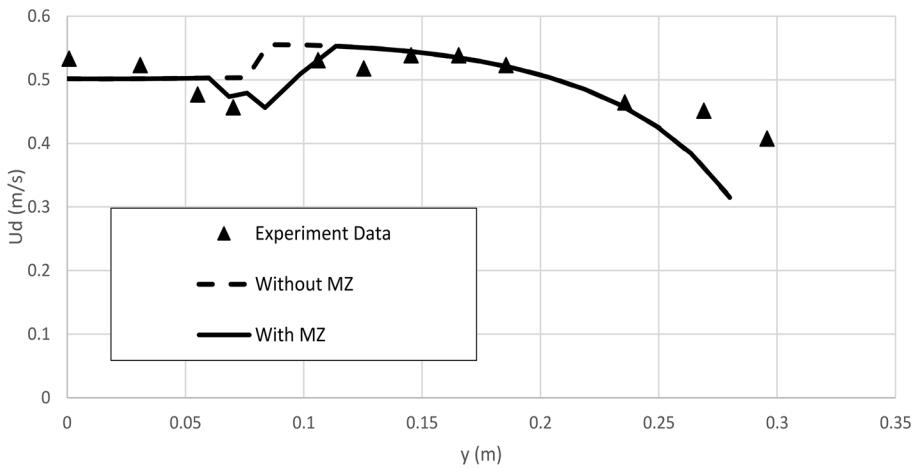


Fig. 9 DWK0406 depth-averaged velocity comparison between models with and without MZ model

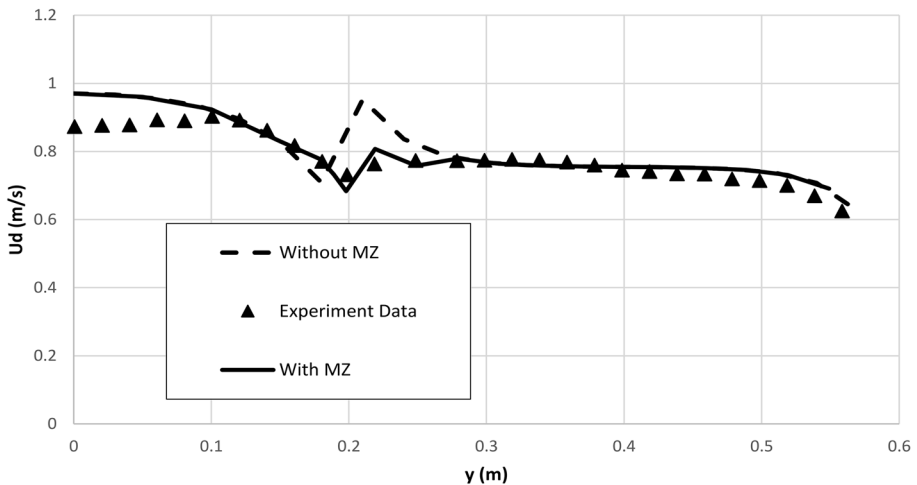


Fig. 10 ROS255 depth-averaged velocity comparison between models with and without MZ model

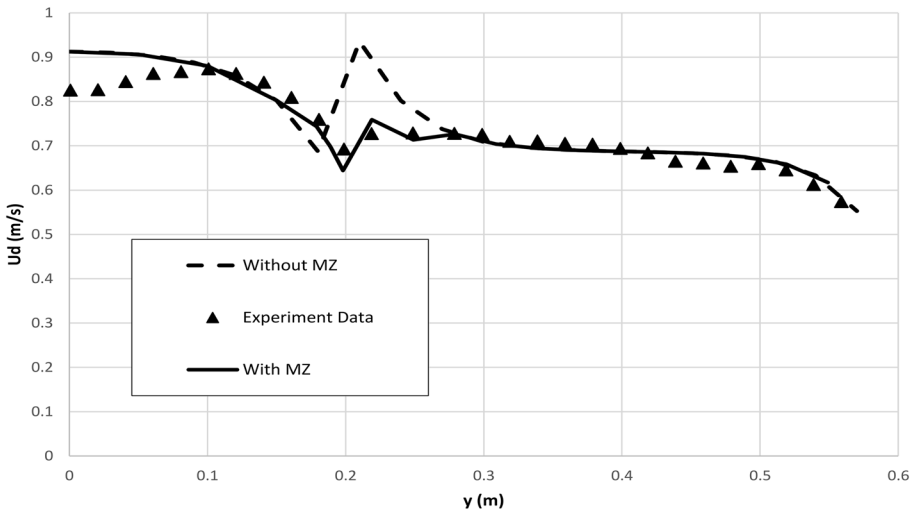


Fig. 11 ROS250 depth-averaged velocity comparison between models with and without MZ model

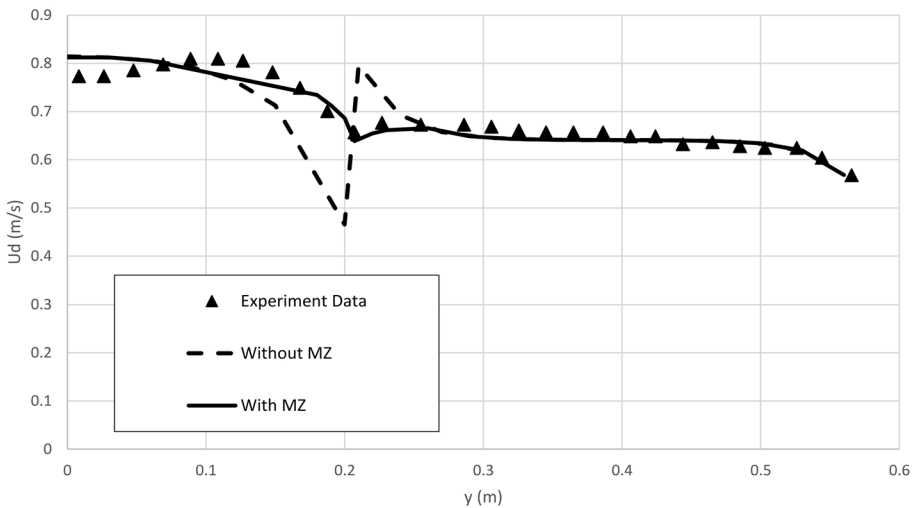


Fig. 12 ROS245 depth-averaged velocity comparison between models with and without MZ model

For validation, it can be observed from Figs. 9, 10, 11, 12 and 13 that for all compound channel flow cases tested, the conventional model without considering MZ approach shows inaccuracy in calculating the flow velocity at the main-channel and floodplain interface region due to the mis-interpretation of secondary current intensity. This interface zone velocity profile modelling has been improved by the present MZ model as benchmarked by the UK-FCF experimental data. Table 4 shows the root-mean square error (RMSE) comparison for interface zone’s velocity calculations with and without MZ approach benchmarked by the measured data. The compared error fraction in the table reveals that the MZ model works better in flow cases with higher velocity, i.e. ROS245, ROS250 and ROS255,

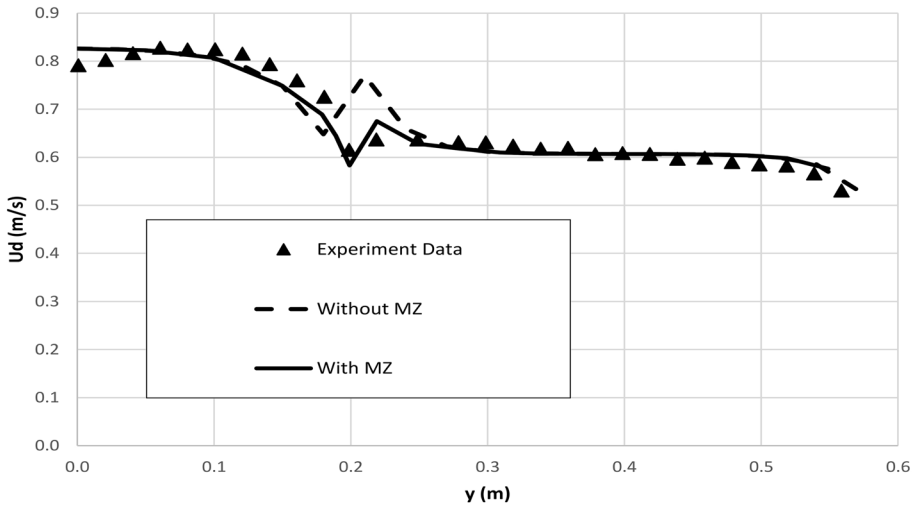


Fig. 13 ROS240 depth-averaged velocity comparison between models with and without MZ model

Table 4 Root-mean square error (RMSE) analysis benchmarked by measured data at the main-channel and floodplain interface region

Test	Width-average of measured velocity (m/s)	Averaged RMSE for calculation Without MZ (m/s)	Averaged RMSE for calculation with MZ (m/s)	Comparative error fraction (non-MZ to MZ model) (–)
DWK0406	0.4968	0.036894	0.013479	2.737
ROS240	0.6737	0.097826	0.033446	2.925
ROS245	0.6922	0.066959	0.012258	5.462
ROS250	0.7381	0.125526	0.028812	4.357
ROS255	0.7834	0.108704	0.031258	3.478

when compared to flows with low velocity. This is due to the fact that those flow cases with higher flow velocity were subjected to more intense secondary current at the interface area, which in terms causing larger differences between MZ and non-MZ models.

The investigated narrow channel flow cases have been influenced by secondary currents which impact the flows towards left and right of the compound step. Compared to wide channel flows, the side-wall and compound step effects are crucial for narrow flow cases and it has been proven that the 2D depth-averaged model could not effectively represent them without combining with innovative approach (i.e. by Nezu and Nakagawa [5], Pu et al. [9], Pu [7]). In the tests of this study, the proposed MZ model has proven to reasonably improve the conventional SKM model deduced from 2D depth-averaged Navier–Stokes flow assumption. It has been shown that by additional sectioning of the flow model laterally, the compound channel 2D modelling accuracy could be improved. Theoretically, the MZ approach works by considering smaller width of the channel sections and hence able to reduce the inaccuracy of SKM

calculation, by reducing error caused by representing whole section with a single simplified Γ .

4 Conclusions

The Shiono–Knight model (SKM) has been investigated to estimate the flow velocity profile within rectangular compound channel which has been subjected to turbulence and secondary flows. Due to its 2D Navier–Stokes assumption, SKM has found to represent the narrow channel flow with less accuracy compared to wide channel flows. A multi-zonal (MZ) approach has been proposed to improve this modelling weakness. In the proposed MZ model, the investigated compound channel flows have been sectioned with extra zones in the interface region between main-channel and floodplain where the escalated secondary flow effect has been considered. To validate the proposed MZ model, it was used to calculate and compare with the experimental data by national UK-FCF facility. The comparison with measured data showed that the proposed MZ model represents the narrow flows with better accuracy than the SKM approach for the rectangular compound channel flow cases. This study has also proven that the modelling of narrow 3D-characterised secondary flow could be improved by considering extra zones’ turbulence and secondary current modelling in the analytical model.

Acknowledgement The help of Ms. Faye Lynch (the author’s former undergraduate student) is greatly appreciated in the model testing and formulations.

OpenAccess This article is distributed under the terms of the Creative Commons Attribution 4.0 International License (<http://creativecommons.org/licenses/by/4.0/>), which permits unrestricted use, distribution, and reproduction in any medium, provided you give appropriate credit to the original author(s) and the source, provide a link to the Creative Commons license, and indicate if changes were made.

References

1. Castanedo S, Medina R, Mendez FJ (2005) Models for the turbulent diffusion terms of shallow water equations. *J Hydraul Eng* 131(3):217–223
2. Ervine DA, Babaeyan-Koopaei K, Sellin RHJ (2000) Two-dimensional solution for straight and meandering overbank flows. *J Hydraul Eng* 126(9):653–659
3. Liao H, Knight DW (2007) Analytic stage-discharge formulas for flow in straight prismatic channels. *J Hydraul Eng* 133(10):1111–1122
4. Liao H, Knight DW (2007) Analytic stage-discharge formulae for flow in straight trapezoidal open channels. *Adv Water Resour* 30(1):2283–2295
5. Nezu I, Nakagawa H (1993) Turbulent open-channel flows. IAHR Monograph: A.A. Balkema, Amsterdam
6. Nezu I, Tominaga A, Nakagawa H (1993) Field measurements of secondary currents in straight rivers. *J Hydraul Eng* 119:598–614
7. Pu JH (2015) Turbulence modelling of shallow water flows using Kolmogorov approach. *Comput Fluids* 115:66–74
8. Pu JH, Lim SY (2014) Efficient numerical computation and experimental study of temporally long equilibrium scour development around abutment. *Environ Fluid Mech* 14:69–86
9. Pu JH, Shao S, Huang Y (2014) Numerical and experimental turbulence studies on shallow open channel flows. *J Hydro Environ Res* 8:9–19
10. Pu JH, Tait S, Guo Y, Huang Y, Hanmaiahgari PR (2018) Dominant features in three-dimensional turbulence structure: comparison of non-uniform accelerating and decelerating flows. *Environ Fluid Mech* 18(2):395–416

11. Shiono K, Knight DW (1988) Two-dimensional analytical solution for compound channel. In: Proceedings of third international symposium on refined flow modeling and turbulence measurements, Tokyo, Japan, pp 503–510
12. Shiono K, Knight DW (1991) Turbulent open-channel flows with variable depth across the channel. *J Fluid Mech* 222(1):617–646
13. Tang X, Knight DW (2008) A general model of lateral depth-averaged velocity for open channel flows. *Adv Water Resour* 31(1):846–857
14. Tang X, Knight DW (2008) Lateral depth-averaged velocity distributions and bed shear in rectangular compound channel. *J Hydraul Eng* 134(9):1337–1342
15. Tang X, Knight DW (2009) Analytical models for velocity distributions in open channel flows. *J Hydraul Res* 47(4):418–428
16. Van Prooijen BC, Battjes JA, Uijttewaal WSJ (2005) Momentum exchange in straight uniform compound channel flow. *J Hydraul Eng* 131(3):175–183
17. Yang Z, Gao W, Huai W (2010) Secondary flow coefficient of overbank flow. *Appl Math Mech* 31(6):709–718
18. Yang K, Nie R, Liu X, Cao S (2012) Modeling depth-averaged velocity and boundary shear stress in rectangular compound channels with secondary flows. *J Hydraul Eng* 139(1):76–83

Publisher's Note Springer Nature remains neutral with regard to jurisdictional claims in published maps and institutional affiliations.